JCTC Journal of Chemical Theory and Computation

Article

pubs.acs.org/JCTC

Exploration of Protein Conformational Change with PELE and Meta-Dynamics

Benjamin P. Cossins,[†] Ali Hosseini,[†] and Victor Guallar*[,†,‡]

[†]Joint BSC-IRB Research Program in Computational Biology, Barcelona Supercomputing Center, c/Jordi Girona 29,08034 Barcelona, Spain

[‡]Institució Catalana de Recerca i Estudis Avançats (ICREA), Passeig Lluís Companys 23, 08010 Barcelona, Spain

Supporting Information

ABSTRACT: Atomistic molecular simulation methods are now able to explore complex protein or protein−ligand dynamical space in a tractable way with methods such as meta-dynamics or adaptive biasing force. However, many of these methods either require a careful selection of reaction coordinates or the knowledge of an initial pathway of some kind. Thus, it is important that effective methods are developed to produce this pathway data in an efficient fashion. PELE, a proven protein−ligand sampling code, has been developed to provide rapid protein sampling in highly flexible cases, using a reduced network model eigen problem approach. The resulting method is able to rapidly sample configuration space with very general driving information. When applied to ubiquitin, PELE was able to reproduce RMSD and average force data found in molecular dynamics simulations. PELE was also applied to explore the opening/closing transition of T4 lysozyme. A meta-dynamics exploration using a low energy pathway validated that the configurations explored by PELE represent the most populated regions of phase space. PELE and meta-dynamics explorations also discovered a low free energy region where a large cross-domain helix of T4 lysozyme is broken in two. There is previous NMR evidence for the validity of this unfolded helix region.

1. INTRODUCTION

Recent years have brought the realization of important milestones in atomistic protein simulation. Simulations of relatively large time scale events such as protein folding, protein−ligand association, and large scale conformational change are becoming tractable and predictive.[1−5] These advances rely on accelerated methods which use simplified pathway coordinates to explore complex many-dimensional processes and/or molecular simulation techniques able to efficiently use large numbers of computer processors.[6,7] Whatever the combination of methods used, there is a need to perform hundreds of nanoseconds worth of conformational sampling. The scale of computer power needed for systems of interest is not available to all, and so for the majority, the problem of rapidly obtaining realistic dynamic information on proteins remains.

Methods able to quickly probe large scale protein conformational changes based on molecular dynamics such as steered MD[8,9] (SMD) and essential dynamics sampling (EDS))[10−12] have been used to direct MD in a direction of interest through clever constraints or restraints. There are many examples of steered or biased MD simulations being used to find a pathway for further free energy analysis with umbrella sampling or other such methods.[9,13,14] A recently developed method, temperature-enhanced essential dynamics replica exchange, seems able to steer large biomolecular MD simulations through temperature control of specific essential space modes while maintaining Boltzmann weighting.[15] Other advanced methods such as the finite temperature string method[16] and transition path sampling[17,18] attempt to sample defined pathways using molecular dynamics.

Alternative pathway building methods have been developed based on minimization rather than MD. A family of methods based on the nudged elastic band method (NEB)[19−22] have been used to find pathways between two experimental structures of the same protein. NEB methods in general work on the basis of the minimization of a series of intermediate configurations between two end point protein structures. Every intermediate configuration is connected to the previous and next by springs which keep the structure of the path while allowing minima to be found. NEB methods have been used to find probable low energy pathways of protein conformational change, which can then be used in conjunction with free energy methods to give predictive information.[23]

We present here a novel methodology capable of producing accurate and quick conformational sampling, and of providing reliable initial pathways for free energy methods. The methodology is a new development of the Protein Energy Landscape Exploration (PELE) program. PELE, a Monte Carlo (MC) based method, has thus far been used to characterize the exit pathways of bound molecules from proteins and for protein−ligand docking.[24−26] We introduced a new protein perturbation step based on anisotropic network model methodologies, capable of providing significant backbone motion.

These PELE developments have been tested on two systems: ubiquitin (Ubi) and T4 lysozyme (T4lyz). Both systems were chosen due to their small size and the amount of experimental and computational studies on their dynamics. For Ubi, a 76 residue regulatory protein, we have compared the PELE

Received: September 25, 2011
Published: January 27, 2012

conformational search with three 1 μs MD trajectories. MD simulations of this length have been shown to map the conformational space of native Ubi, through comparison with NMR data.[27] For T4lyz, an enzyme found in *Escherichia coli* (*E. coli*), which has been infected with the bacteriophage T4, we perform meta-dynamics calculations[28,29] using a pathway defined after a PELE exploration of the opening and closing pathways of the two domains presents in T4lyz.

2. METHODS

2.1. Anisotropic Network Model (ANM) driven PELE. The methodology has been built on the foundations of the PELE program which has thus far been used to characterize ligand exit pathways from proteins.[24−26] PELE uses a Monte Carlo (MC) scheme where new trial configurations are produced with sequential system perturbation, side chain prediction, and minimization steps. Trial configurations are then filtered with a Metropolis acceptance test. Using the MPI protocol, multiple trajectories can produce simultaneous trial configurations that share information and interchange coordinates toward one common goal.

2.1.1. Perturbation Step. Previous PELE studies used ligand translation and rotation for the perturbation step. Now, a protein perturbation step has been added to the PELE MC scheme that uses a reduced harmonic model of the system to calculate the probable major motions. The reduced harmonic model and the application of the calculated motions to perturb the system can take a number of forms.

α-Carbon ANM Perturbation. The initial reduced harmonic model used was the α-carbon anisotropic network model (PELE-CA) similar to that described by Tirion.[30] The PELE-CA model uses the α-carbons (CAs) to create a network model with identical springs connecting all CAs within a predefined cutoff (15 Å for PELE-CA in this study). A decay parameter (2.5 for PELE-CA in this study) is also included such that the force constant of the PELE-CA springs is decreased with the interaction distance. A similar decay parameter has been shown to improve the accuracy of ANM models in a recent study.[31] Extra user defined atoms and/or automatically chosen atoms from any ligand can also be included in the network. The Hessian matrix diagonalization of this reduced harmonic potential results in a series of eigenvectors that have been shown to describe the vibrational dynamics of proteins and their complexes.[32,33] Of course, for this model, movement vectors are acquired only for CAs. Thus, PELE-CA calculated motions are applied to the all atom (AA) system through the addition of harmonic restraints to CAs in the directions of the chosen PELE-CA modes. The system is then minimized for this biased potential, which has the effect of moving the system in the desired direction. A prototype version of this PELE-CA methodology has been used with success in a recent study of ligand migration in a truncated hemoglobin.[25]

Heavy-Atom ANM Model. A more elaborate alternative reduced harmonic model has been developed which uses all heavy atoms (HAs) of the AA system to create an elastic network model (PELE-HA). Pairs of HAs which have covalent or disulfide bonds between them are given a very high force constant spring (300 kcal mol^{-1}) while nonbonded HA pairs are given a spring with a far weaker force constant (0.5 kcal mol^{-1}; HA pairs more distant than 50 Å are not included). This model has similarities to recently published ANM and GNM models.[34,35] Again, a force constant decay parameter is applied such that longer springs are softer (3 for PELE-HA in this study). This more complex harmonic model gives more detailed protein motions; however, these motions are calculated more slowly (2−10 s for PELE-CA and 2 min for PELE-HA on a 2000 atom system).

For the PELE-HA model, movement vectors are acquired for all heavy atoms. Hydrogen movement vectors are found by copying the vectors of atoms to which the hydrogens in question are covalently bonded. For this AA perturbation scheme, the system is not minimized with a biased potential following a chosen mode, as performed in the PELE-CA. Perturbation steps along given vectors are directly applied on all atoms, followed by a minimization where we constrain all CAs to the final perturbed position. Additionally, PELE-HA uses a nested-move consisting of a large number (50) of small randomly directed moves with move sizes scaled by the eigenvalue of the mode. Nested moves with an energy above a simple predefined threshold are rejected; however, in practice almost all moves are accepted. Of course the final trial configuration may be rejected by the acceptance test at the end of the PELE step.

Choosing ANM Modes. The problem of which ANM modes to apply is solved in a number of different ways. Single ANM modes or combinations can be chosen at random from a range of 1 to N modes where only these N modes are calculated to save time. This random sampling of modes can also be biased by the frequency of the modes such that the lowest frequency modes are chosen more often. In this study, modes were chosen at random from the top 10 (N = 10) for PELE-CA and from the top 50 (N = 50) using a biased distribution for PELE-HA.

The magnitude of the displacement down the calculated movement vectors can also be chosen at random from a predefined range of distances which can be biased by the frequency of the modes in question such that lower frequency modes use larger displacements. Of course in the case of PELE-CA, displacements discussed here are in fact the length of applied harmonic restraints.

If a target structure is provided, a PELE simulation can move toward this target. This is achieved by picking ANM modes which display a predefined level of directional overlap with the vectors of each atom of the initial structure to the equivalent atoms of the target. Directional overlap is simply the dot product of the mode vector with the vectors to the target structure. A random number can then be used to discard some overlapping modes such that sequential trials have differing overlapping modes. When a target structure is not available the spawning methodology of PELE is applicable, as described below in the Minimization Step section.

2.1.2. Side Chain Step. Due to larger protein motion, as a result of the new perturbation, the side-chain optimization step has been developed to pick residues which underwent a large energy change along the perturbation. Each side chain residue energy is computed before and after the perturbation. Thus, the user can choose side chains with the largest energy increase (top residues) and predict a better side chain position (using the algorithms developed in the PLOP program[36]). There is also the option to choose fewer top residues and select a spherical cluster around them. The user can control the number of high-energy residues optimized and the radius of the clusters around these residues. In this study, all PELE searches used two high energy residues and clusters with radii of 3 Å. In our experience, the number of side chains to be optimized should not exceed 25. Due to the approximate (but quicker) side chain

prediction algorithms, larger groups of side chains will result in high energy states and a low Metropolis acceptance.

2.1.3. Minimization Step. The last step in the PELE sampling algorithm uses a truncated Newton minimization of all of the system (or of those parts of the system included in the first two steps). While the minimization allows us to attain energetically accessible regions, it might also revert the structure to the initial conditions. In order to improve the conformational sampling, we have added the possibility to constrain the CAs to their final perturbed position within the final minimization. After this minimization, the trial configuration is accepted or rejected as stated above.

The multiprocessor parallel implementation of PELE shares predefined metrics across identical replica calculations. For example, several processors running identical PELE calculations can perform a random search with ANM protein sampling, those which manage to move away from an initial structure will export their coordinates to the processors lagging behind (within a given threshold).[24] This multiprocessor structure is able to drive the sampling to find new low energy configurations away from the initial. This "spawning" algorithm can be used to drive many different metrics. In this study, one of our spawning criteria for T4Lyz is the distance between the α-carbons of GLU22 and ARG137. Hence, a multiprocessor search would allow all processors to search the conformational space of T4Lyz randomly until one processor has a GLU22-ARG137 distance which is 4 Å smaller than the largest GLU22-ARG137 distance found. At this point, the processor with the smallest GLU22−ARG137 distance takes on the configuration with the largest GLU22−ARG137 distance and continues to search.

2.2. Free Energy Methods. Meta-dynamics is a free energy methodology developed by the Parrinello group and is able to explore the free energy differences of atomistic systems using a series of driving collective variables. Here, we use meta-dynamics to explore the pathways found with PELE as a form of validation. A very brief description of meta-dynamics follows; more information can be found in various reviews.[29,37]

The concept of meta-dynamics is based around finding a collective variable of a system which, in a coarse-grained fashion, describes a property of interest within a simulation. Gaussians of width σ_i are then added to the collective variable in a history dependent manner such that the system is less likely to return to a region of the collective variable which has already been explored. The free energy surface of the region explored can then be found through the negative of the total biasing potential which was added through the simulation.

More recent developments of meta-dynamics (well tempered meta-dynamics) have given the possibility of faster and more complete convergence[38,39] through the adaptive adjustment of the Gaussian deposition rate ω, achieved by rescaling W, the height of Gaussians.

Another development by the same group provides two functions of a possible reaction coordinate R which allow for efficient exploration of otherwise complex collective variables:[28]

$$s(R) = \lim_{\lambda\to\infty} \frac{\int_0^1 t e^{-\lambda(R-R(t))^2}\,dt}{\int_0^1 e^{-\lambda(R-R(t))^2}\,dt} \quad (1)$$

and

$$z(R) = \lim_{\lambda\to\infty} -\frac{1}{\lambda}\ln\int_0^1 e^{-\lambda(R-R(t))^2}\,dt \quad (2)$$

In our case, R is a series of protein α-carbon coordinates for conformations of a protein which describe the motion of interest and $(R - R(t))^2$ is the mean square displacement between the present configuration and the defined path. For sufficiently large λ, these functions allow a meta-dynamics search of the path defined by R such that the s path defines the distance along R and the z path defines the distance from R. In this way, a representation of the free energy landscape of R and surrounding regions can be calculated through

$$F(s, z) = -\frac{1}{\beta}\ln\left\langle \delta(s - s(R))\delta(z - z(R)) \right\rangle \quad (3)$$

2.3. Simulation Setup. T4lyz and Ubi structures used were PDB codes 3DMV and 1AAR, respectively. For T4lyz, all heteroatoms including ligands, ions, and water were removed, hydrogens were added, and HIS 31 was protonated at both the Δ and ε positions. For Ubi, again all heteroatoms were removed, hydrogens were added, and no residues received extra protons. The structures were then minimized with constrained α-carbons using a truncated-Newton algorithm and SGB solvation of PLOP.[36]

The MD simulation of Ubi was performed with GROMACS 4.0.5.[6] and three different force fields: OPLSAA, Amber, and Charm. The system was solvated with a periodic cubic box, containing 8813 TIP3P[40] molecules and particle mesh Ewald (PME) long-range electrostatics.[41] Lennard-Jones interactions were cut off at 9 Å with a switching function, and Coulomb interactions were cut off at 10 Å. Temperature and pressure equilibrations preceded the 1 μs of production at 300 K and 1 atm where system configurations were saved every 10 ps.

Meta-dynamics simulations were performed with GROMACS 4.0.5 patched with Plumed.[42] The OPLSAA force-field was used along with PME and similar cutoff and equilibration arrangements to the GROMACS simulations described above.

3. RESULTS

In order to study the capabilities of PELE being able to reproduce local fluctuations, PELE-CA and PELE-HA explorations of Ubi have been compared to molecular dynamics. Eight processors were allowed to freely explore (no search guidance) conformations around the initial structure for 24 h; an additional 24 h did not produce any significant change. Modes were chosen randomly from the top 50 in terms of frequency, and move sizes had a maximum of 1.5 Å and were biased not to be too small.

Figure 1 shows the RMSD from the initial structure for individual residues from PELE and three 1 μs (each with a different force field) explicitly solvated MD simulations. While there are a few differences for most residues, in particular between the different force fields, there is an overall quantitative agreement. Remarkably, PELE captures most of the maximum and minimum fluctuations at a fraction of the MD cost. This agreement can also be seen when comparing average atomistic simulation forces. Bond length forces are of course very different owing to the minimization of PELE. Nonbonded, 1−4 interaction, torsional, and angle forces are very similar to those seen in Figure 2 and the Supporting

dx.doi.org/10.1021/ct200675g | J. Chem. Theory Comput. 2012, 8, 959−965

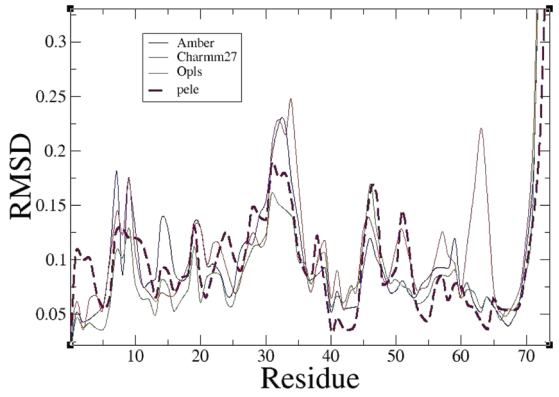

Figure 1. Plot of residue RMSD to average structures for MD using the OPLSAA, AMBER, and CHARMM27 force fields and OPLSAA PELE simulations of ubiquitin.

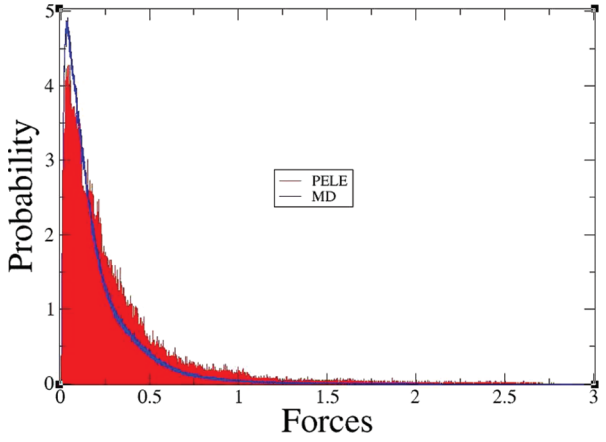

Figure 2. Histograms of atomistic nonbonded forces from PELE (red) and MD (blue).

Information. These comparisons suggest that the conformational space explored by PELE is very similar to that of MD.

Table 1 shows the results of a cluster analysis of PELE and MD ubiquitin trajectories. As seen when comparing PELE with MD, but also when comparing the different MD force fields, all simulations produce a similar number of clusters and agree on the percentage population of the top 4 and top 1 cluster. It is remarkable that PELE, a quick exploration technique with approximately 2 orders of magnitude less computational cost, can reproduce this semiquantitative analysis. Additionally, PELE has the most clusters with a 2 Å cutoff, suggesting that PELE finds more significantly different conformations.

Both PELE-CA and PELE-HA protocols as defined in the Methods section were applied to open T4lyz. After the initial minimization, PELE starts with a local exploration (100 iterations of free search) of the initial closed structure in order to relax the system. Then, searches of the opening process using driving metrics were performed. PELE-CA and HA searches used spawning on energy and atom−atom distance (GLU22 and ARG137 α-carbons). Once fully opened, with an α carbon RMSD of 5 Å from the initial structure, another short local search of the opened structure is carried out. Then, the driving metrics are reversed, and searches return toward the initial structure.

PELE-CA and -HA searches using 32 processors and drawing modes from the top 50 biased by frequency were able to open and close T4Lyz 1−2 times in 48 h. The potential energy data (Figure 3) seem to suggest low energy regions at the closed and open states. The energy profile clearly indicates that PELE-CA and -HA calculations seem very similar and essentially provide the same trajectories. Figure 4 shows the projection of the conformers of the PELE-HA trajectory on the PCA vectors calculated from the same trajectories. The opening−closing motion is very clear in vector 1, and there seems to be a small correlation with this motion for vectors 2 and 5. For the other PCA vectors, there seems to be more of a relaxation through the simulation. For these PELE trajectories, the eigenvalue of the first PCA vector is 20 times larger than any other, and this is borne out in the projection analysis (Figure 4). A visual comparison of the PCA vectors calculated for both PELE-CA and -HA and those found through a similar procedure using MD[43] suggested a good level of similarity.

The red circles in the HA plots of Figure 3 show the configurations chosen by binning all configurations by RMSD to the initial and choosing the lowest energy configuration in each bin. These configurations were visualized and assessed to ensure maximal equality in RMSD between all. If a chosen configuration was deemed to be too far from the required RMSD equality, it was removed, and the gap was filled using the Morph Server of Krebs and Gerstein.[44] The four open T4lyz structures with the same structure as that used here (150 L)[45] were within 1.3 Å of one of the configurations of the final pathway used in the meta-dynamics analysis. PELE projected these conformations without any previous knowledge of the open structure.

Figure 5 shows the free-energy landscape around the pathway taken from the PELE search. The x axis shows the S-path (see eq 1), which starts at 4 and ends at 7.5 units. The y axis shows the Z-path (see eq 2), which describes the distance from the S-path in Å^2. Figure 6 shows graphic representations of the important regions found in Figure 5. The lowest free-energy regions (regions 1−3) of phase space were found close to the path found by PELE and correspond directly to the low energy regions in Figure 3. The two lowest energy regions suggest that T4Lyz is able to open and close with energy barriers of around 10 and 30 kJ mol^{-1}, respectively.

Table 1. Table of Results for a Series of Cluster Analyses of Ubiquitin Trajectories Using PELE and MD with Different Force Fields[a]

	PELE			MD:OPLS			MD:AMBER			MD:CHARMM		
cutoff (Å)	1	1.5	2	1	1.5	2	1	1.5	2	1	1.5	2
no. of clusters	98	19	8	238	20	6	157	14	4	110	12	4
% in top 4 clusters	39	86	95	38	88	99	44	96	100	60	96	100
% in top cluster	17	56	80	14	60	97	14	56	86	34	63	96
no. clusters for 90% of frames	33	5	2	54	4	1	28	4	2	16	2	1

[a]This analysis was carried out with the gcluster GROMACS[6] tool, using the linkage algorithm and α-carbon RMSD.

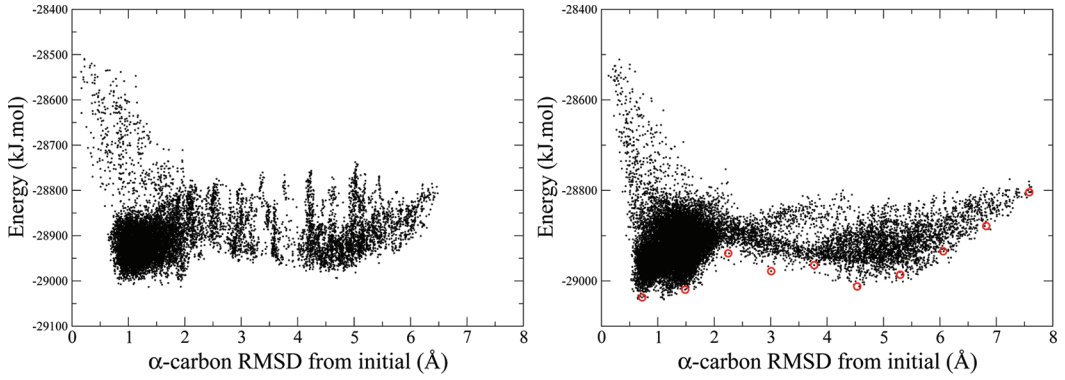

Figure 3. Potential energy against α-carbon RMSD from the initial structure for (a) PELE-CA and (b) PELE-HA searches targeted with spawning on α-carbon RMSD and atom. Red circles represent configurations chosen by the low energy binning procedure and used to create the meta-dynamics path after visual analysis.

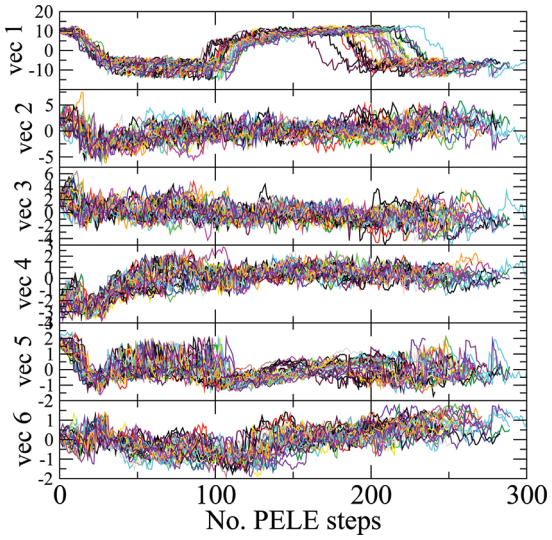

Figure 4. Projections (in nm) of PELE-HA trajectories on their PCA eigenvectors. Each PELE MPI process is colored differently. The PELE search started in the closed state; hence, the vec1 plot 10 correspends to the closed state and −10 to the open state.

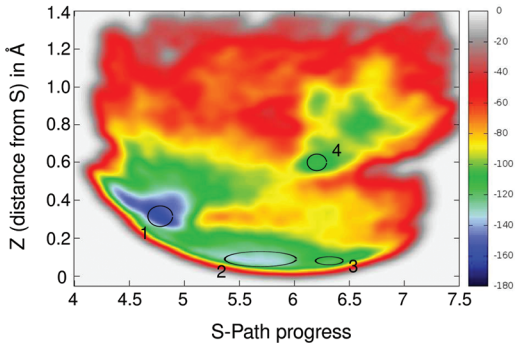

Figure 5. Free energy map of the PELE pathway and surrounding region explored using meta-dynamics. The free energy is depicted by color in kJ mol^{-1}.

Additionally, the large cross domain helix was found to break in the most open conformations (region 3), and this helix was found to become even more broken in an isolated region, which may not be significantly populated (region 4).

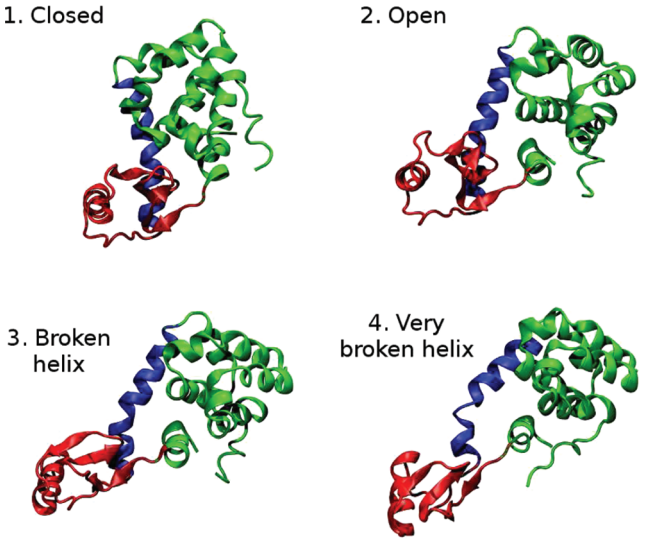

Figure 6. T4Lyz structures representing the different states found in the meta-dynamics analysis and referenced in Figure 5.

4. DISCUSSION

Combining protein structure prediction algorithms with a Monte Carlo sampling technique, we introduced PELE, a program capable of describing the protein energy landscape associated with ligand migration in proteins. By adding a backbone perturbation following normal modes, we have expanded these capabilities to explore local dynamics and large conformational changes. A comparison of residue based RMSD and average force decomposition for Ubi suggests that PELE can rapidly give an idea of the protein conformational space. Employing the spawning methodology, PELE was able to rapidly explore the large conformational space of T4lyz.

Both PELE-CA and PELE-HA seem suitable for the purposes of rapid exploration of protein large conformational change and fully explored the open/close transitions in T4Lyz in just 1−2 days usage of a small cluster. The minimum RMSD between the pathway denoted by red circles in Figure 3 and the open and closed states in Figure 6 was 1.55 Å and 1.80 Å, respectively. We should emphasize that PELE projected the open conformation, and the pathway toward it, without any knowledge of the open structure. As stated, the conformational exploration used the GLU22 and ARG137 atom distance as

dx.doi.org/10.1021/ct200675g | J. Chem. Theory Comput. 2012, 8, 959−965

spawning criteria. Equivalent results, however, were obtained when using as spawning criteria the RMSD to the initial structure, indicating the robustness of the landscape and of the search procedure. The overall method could be very useful as in the absence of initial pathway information, MD would need significant computational resources. The low free-energy regions of T4Lyz phase-space found by meta-dynamics were very similar to the low potential energy pathway found by PELE. However, if accurate free energies are necessary, then PELE should be combined with another more rigorous exploration technique and possible experimental methods.

Our calculations suggest that the main cross-domain helix is broken as T4Lyz becomes more open. This helix becomes slightly broken at the extremity of the probably well populated open region (region 3 of Figure 3) and very broken in the little populated region 4. Any functional significance is not clear, but there is experimental NMR evidence based on a loss of stability and hydrogen bonds in the helix.[46,47] Another simulation analysis of T4Lyz[43] has been carried out, and although this study only uses 1 ns trajectories, the PCA analysis provides similar modes and eigenvalues to those found in the present study and analyzed in the PCA projection analysis. While there is some controversy, experimental studies[48,49] seem to suggest that, in solution, T4lyz is generally more open than closed. Our energy profiles indicate a larger basin (and more minima) for the open state. Using the OPLS-AA force field, however, the closed state is 3 kcal mol^{-1} more stable. Thus, it is difficult to predict the preferred state of the system without a kinetic analysis (which is not the aim of this study).

The protein sampling capabilities of PELE are an addition to the molecular modeling tool-kit, which allows rapid sampling of interesting protein motions on the atomistic scale. These capabilities are complemented well by those of meta-dynamics, but PELE is also useful for any application which requires protein sampling such as protein−ligand and protein−protein docking. A public Web server for PELE protocols will be made available in January 2012 at http://pele.bsc.es.

■ ASSOCIATED CONTENT

Supporting Information

A series of histograms comparing atomistic forces from PELE and MD simulations of ubiquitin. This material is available free of charge via the Internet at http://pubs.acs.org.

■ AUTHOR INFORMATION

Corresponding Author

*E-mail: victor.guallar@bsc.es.

Notes

The authors declare no competing financial interest.

■ ACKNOWLEDGMENTS

The authors would like to thank Santi Esteban-Martin and Xavier Salvatella for helpful discussions and for supplying some MD trajectories of ubiquitin. Also the European Research Council for grant ERC-2009-Adg 25027-PELE.

■ REFERENCES

(1) Piana, S.; Laio, A. *J. Phys. Chem. B* **2007**, *111*, 4553−4559.
(2) Kubitzki, M. B.; de Groot, B. L. *Structure* **2008**, *16*, 1175−1182.
(3) Pietrucci, F.; Marinelli, F.; Carloni, P.; Laio, A. *J. Am. Chem. Soc.* **2009**, *131*, 11811−11818.
(4) Berteotti, A.; Cavalli, A.; Branduardi, D.; Gervasio, F. L.; Recanatini, M.; Parrinello, M. *J. Am. Chem. Soc.* **2009**, *131*, 244−250.
(5) Lemkul, J. A.; Bevan, D. R. *J. Phys. Chem. B* **2010**, *114*, 1652−1660.
(6) Spoel, D. D.; Lindahl, E.; Hess, B.; Groenhof, G.; Mark, A. E.; Berendsen, H. J. C. *J. Comput. Chem.* **2005**, *26*, 1701−1718.
(7) Bowers, K. J.; Chow, E.; Xu, H.; Dror, R. O.; Eastwood, M. P.; Gregersen, B. A.; Klepeis, J. L.; Kolossváry, I.; Moraes, M. A.; D., F.; Salmon, J. K.; Shan, Y.; Shaw, D. E. *Proc. ACM/IEEE Conf. Supercomput.* **2006**.
(8) Shen, L.; Shen, J.; Luo, X.; Cheng, F.; Xu, Y.; Chen, K.; Arnold, E.; Ding, J.; Jiang, H. *Biophys. J.* **2003**, *84*, 3575−3590.
(9) Cuendet, M. A.; Michielin, O. *Biophys. J.* **2008**, *95*, 3575−3590.
(10) Amadei, A.; Linssen, A. B. M.; Berendsen, H. J. C. *Proteins: Struct., Funct., and Bioinf.* **1993**, *17*, 412−425.
(11) Amadei, A.; Linssen, A. B.; de Groot, B. L.; van Aalten, D. M.; Berendsen, H. J. *J. Biomol. Struct. Dyn.* **1996**, *13*, 615−625.
(12) Daidone, I.; Amadei, A.; Roccatano, D.; Nola, A. D. *Biophys. J.* **2003**, *85*, 2865−2871.
(13) Liu, Z.; Xu, Y.; Tang, P. *J. Phys. Chem. B* **2006**, *110*, 12789−12795.
(14) Huang, H.; Ozkirimli, E.; Post, C. B. *J. Chem. Theory Comput.* **2009**, *5*, 1304−1314.
(15) Kubitzki, M. B.; de Groot, B. L. *Biophys. J.* **2007**, *92*, 4262−4270.
(16) Vanden-Eijnden, E.; Venturoli, M. *J. Chem. Phys.* **2009**, *130*, 194103.
(17) Dellago, C.; Bolhuis, P. G.; Chandler, D. *J. Chem. Phys.* **1999**, *110*, 6617.
(18) Bolhuis, P. G.; Chandler, D.; Dellago, C.; Geissler, P. L. *Annu. Rev. Phys. Chem.* **2002**, *53*, 291−318.
(19) Elber, R.; Karplus, M. *Chem. Phys. Lett.* **1987**, *139* (380), 375.
(20) Fischer, S.; Karplus, M. *Chem. Phys. Lett.* **1992**, *194*, 252−261.
(21) Henkelman, G.; Uberuaga, B. P.; Jonsson, H. *J. Chem. Phys.* **2000**, *113*, 9901−9904.
(22) Ignacio Fdez. Galvin, F.; Field, M. J. *J. Comput. Chem.* **2008**, *29*, 139−143.
(23) Arora, K.; Brooks, C. L. *Proc. Natl. Acad. Sci. U.S.A.* **2007**, *104*, 18496−18501.
(24) Borrelli, K. W.; Vitalis, A.; Alcantra, R.; Guallar, V. *J. Chem. Theory Comput.* **2005**, *1*, 1304−1311.
(25) Guallar, V.; Lu, C.; Borrelli, K.; Egawa, T.; Yeh, S. *J. Biol. Chem.* **2009**, *284*, 3106−3116.
(26) Borrelli, K. W.; Cossins, B.; Guallar, V. *J. Comput. Chem.* **2010**, *31*, 1224−1235.
(27) Lange, O. F.; van der Spoel, D.; de Groot, B. L. *Biophys. J.* **2010**, *99*, 647−655.
(28) Branduardi, D.; Gervasio, F. L.; Parrinello, M. *J. Chem. Phys.* **2007**, *126*, 054103.
(29) Leone, V.; Marinelli, F.; Carloni, P.; Parrinello, M. *Curr. Opin. Struct. Biol.* **2010**, *20*, 148−154.
(30) Tirion, M. M. *Phys. Rev. Lett.* **1996**, *77*, 1905−1908.
(31) Eyal, E.; Yang, L.; Bahar, I. *Bioinformatics (Oxford, England)* **2006**, *22*, 2619−2627.
(32) Bahar, I.; Atilgan, A. R.; Erman, B. *Folding Des.* **1997**, *2*, 173−81.
(33) Atilgan, A. R.; Durell, S. R.; Jernigan, R. L.; Demirel, M. C.; Keskin, O.; Bahar, I. *Biophys. J.* **2001**, *80*, 505−15.
(34) Lu, M.; Ma, J. *Proc. Natl. Acad. Sci. U.S.A.* **2008**, *105*, 15358−15363.
(35) Rueda, M.; Bottegoni, G.; Abagyan, R. *J. Chem. Inf. Model.* **2009**, *0*, 358−363.
(36) Jacobson, M. P.; Friesner, R. A.; Xiang, Z.; Honig, B. *J. Mol. Biol.* **2002**, *320*, 597−608.
(37) Laio, A.; Gervasio, F. L. *Rep. Prog. Phys.* **2008**, *71*, 126601.
(38) Barducci, A.; Bussi, G.; Parrinello, M. *Phys Rev Lett.* **2008**, *100*, 020603.
(39) Bonomi, M.; Barducci, A.; Parrinello, M. *J. Comput. Chem.* **2009**, *30*, 1615−1621.
(40) Price, D. J. III; C., L. B. *J. Chem. Phys.* **2004**, *121*, 10096−10103.

(41) Darden, T.; Perera, L.; Li, L.; Pedersen, L. *Structure* **1999**, *7*, R55−R60.
(42) Bonomi, M.; Branduardi, D.; Bussi, G.; Camilloni, C.; Provasi, D.; Raiteri, P.; Donadio, D.; Marinelli, F.; Pietrucci, F.; Broglia, R. A.; Parrinello, M. *Comput. Phys. Commun.* **2009**, *180*, 1961−1972.
(43) de Groot, B. L.; Hayward, S.; van Aalten, D. M.; Amadei, A.; Berendsen, H. J. *Proteins: Struct., Funct., Bioinf.* **1998**, *31*, 116−127.
(44) Krebs, W. G.; Gerstein, M. *Nucleic Acids Res.* **2000**, *28*, 1665−1675.
(45) Zhang, X.; Matthews, B. *Protein Sci.* **1994**, *3*, 1031−1039.
(46) McIntosh, L. P.; Wand, A. J.; Lowry, D. F.; Redfield, A. G.; Dahlquist, F. W. *Biochemistry* **1990**, *29*, 6341−6362.
(47) Llinas, M.; Gillespie, B.; Dahlquist, F. W.; Marqusee, S. *Nat. Struct. Mol. Biol.* **1999**, *6*, 1072−1078.
(48) Mchaourab, H. S.; Oh, K. J.; Fang, C. J.; Hubbell, W. L. *Biochemistry* **1997**, *36*, 307−316.
(49) Goto, N. K.; Skrynnikov, N. R.; Dahlquist, F. W.; Kay, L. E. *J. Mol. Biol.* **2001**, *308*, 745−764.